

# Heteropoly compounds in ammoxidation of methylpyrazine

V.M. Bondareva, T.V. Andrushkevich, L.G. Detusheva and G.S. Litvak

Federal Scientific Center "Boreskov Institute of Catalysis", pr. Akad. Lavrentieva 5, Novosibirsk 630090, Russia

Received 29 June 1995; accepted 28 August 1996

Catalytic properties of molybdophosphoric, mixed vanadium molybdophosphoric heteropoly acids  $H_{3+n}PMo_{12-n}V_nO_{40}$  ( $n = 0, 1, 2$ ) and their salts  $Na_7PV_4Mo_8O_{40}$  and  $Na_8HPV_6Mo_6O_{40}$  have been studied in methylpyrazine ammoxidation. Partial vanadium substitution for molybdenum in heteropoly acids increases activity and selectivity towards cyanopyrazine. Sodium salts are somewhat less active and selective.

**Keywords:** ammoxidation; methylpyrazine; cyanopyrazine; heteropoly compounds

## 1. Introduction

A unique combination of acid–basic and redox properties of Mo-, W- and V-containing heteropoly acids (HPA) and of heteropoly salts (HPS) provides their wide application in homogeneous and heterogeneous catalysis [1–3]. Actually, the range of HPA and HPS applications encompasses, for instance, liquid-phase homogeneous reactions such as condensation [4], esterification [5], etc. as well as heterogeneous vapor-phase oxidative dehydrogenation [6]. Studies on the oxidation of organic compounds are also numerous and very fruitful. So far in Japan a commercial production of methacrylic acid occurs via methacrolein oxidation over P–Mo–V HPA [7]. HPA and HPS are successfully used in the liquid-phase reactions of fine organic synthesis (FOS) for the production of antioxidants, medicines, vitamins, etc. [8]. Therefore, it is of importance to enhance the studies on catalysis with solid HPA and HPS in FOS.

Forni [9] suggests to produce amidopyrazine, an anti-tubercular medicine, via a heterogeneous-catalytic ammoxidation of methylpyrazine and further hydrolysis of cyanopyrazine obtained. Data on methylpyrazine ammoxidation are few, and concern oxide catalysts [9–12] only.

In the present pioneer study we report on the performance of P–Mo and P–Mo–V heteropoly compounds in the catalytic ammoxidation of methylpyrazine.

## 2. Experimental

We have studied  $H_{3+n}PV_nMo_{12-n}O_{40}$  HPA ( $n = 0, 1, 2$ ) and  $Na_7PV_4Mo_8O_{40}$ ,  $Na_8HPV_6Mo_6O_{40}$  HPS. We failed to obtain free acids containing more than three vanadium atoms, since it was impossible to compensate completely the negative charge, forming in vanadium substitution for molybdenum, by protons.

In order to obtain  $H_3PMo_{12}O_{40}$  solution, commercial HPA was purified by ether extraction.  $H_{3+n}PV_nMo_{12-n}O_{40}$  solutions were prepared boiling  $NaH_2PO_4 \cdot 2H_2O$ ,  $Na_2MoO_4 \cdot 2H_2O$  and  $NaVO_3 \cdot 2H_2O$ , then acidified to pH = 2 and then extracted by ether according to the procedure described elsewhere [13].

In order to prepare Na HPS, containing four or six vanadium atoms, we dissolved  $NaH_2PO_4 \cdot 2H_2O$ ,  $V_2O_5$  and  $MoO_3$  in a boiling water solution of  $NaHCO_3$ , then acidified the solution to pH = 1, and filtered the non-dissolved precipitate.

Solid HPA and HPS were obtained by water evaporation. Thus obtained compounds were dried at 110°C and tabletted. A 0.25–1.00 mm fraction was separated for further studies.

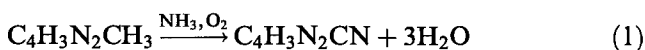
Thermal gravimetric analysis was performed with Derivatograph Q-1500D in air, using a 1 g sample. The heating rate was 10°C per min.

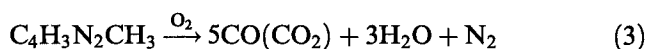
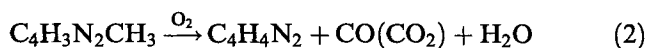
X-ray diffraction patterns were obtained on a D-500 (Siemens) diffractometer with a  $Cu K_\alpha$  monochromatic radiation.

IR spectra were recorded with a Perkin-Elmer 457 spectrometer. Samples (2 mg) were tabletted with CsI.

The catalytic properties were determined in a flow setup with a chromatography analysis of reaction products [14]. Before measurements, the samples were treated in the nitrogen flow at 250°C for 1 h until complete removal of the crystal-hydrate water. All catalysts were exposed to the following reaction mixture:  $C_5H_6N_2 : O_2 : NH_3 : H_2O = 1-2 : 8-10 : 15-20 : 5-7$  (vol%) nitrogen balance. Reaction mixture flow rate was 10 l/h. The reactor (diameter 20 mm) with the catalyst was put into an electric heater with a vibro-fluidized sand bed.

In ammoxidation methylpyrazine (MP) can experience the following transformations:





Here reactions (1), (2) and (3) are respectively the ammoxidation, oxidative dealkylation and complete oxidation of methylpyrazine. Chromatography shows that there is no  $\text{NO}_x$  among the reaction products.

According to eqs. (1)–(3) the selectivities towards cyanopyrazine (CP), pyrazine (P) and carbon oxides were calculated as:

$$S_{\text{CP}}(\%) = \frac{A_{\text{CP}} \times 100}{A_{\text{MP}}^0 - A_{\text{MP}}}$$

$$S_{\text{P}}(\%) = \frac{4A_{\text{P}} \times 100}{5(A_{\text{MP}}^0 - A_{\text{MP}})}$$

$$S_{\text{CO}_x}(\%) = \frac{A_{\text{CO}_x} \times 100}{5(A_{\text{MP}}^0 - A_{\text{MP}})}$$

where  $A_{\text{MP}}^0$  is the inlet methylpyrazine content (moles),  $A_{\text{MP}}$ ,  $A_{\text{CP}}$ ,  $A_{\text{P}}$ ,  $A_{\text{CO}_x}$  are the outlet methylpyrazine, cyanopyrazine, pyrazine and carbon oxides ( $\text{CO} + \text{CO}_2$ ) content (moles), respectively.

The reaction temperature was increased stepwise from 300 to 400°C and the methylpyrazine conversion, reaction products selectivity and carbon balance were determined. In order to compare the catalytic properties of samples, the first-order rate constant of the overall methylpyrazine conversion ( $K^1$  ( $\text{s}^{-1}$ )) and the maximum yield of cyanopyrazine ( $Y(\%)$ ) were calculated.

### 3. Results and discussion

According to the IR data all samples dried at 110°C have the Keggin structure.

#### 3.1. Heteropoly acids $\text{H}_{3+n}\text{PMo}_{12-n}\text{V}_n\text{O}_{40}$

Fig. 1 presents the differential thermal analysis (DTA) curves of the samples. Endothermic peaks within 100–200°C and 350–400°C result from a stepwise dehydration of HPA, accompanied by the loss of crystal-hydrate and structural water, respectively. Chuvayev and coworkers [15] suggested to take the exothermic effect temperature, which follows the structural water loss, as a HPA stability criterion [15].

Studying the P–Mo HPA thermolysis [16], we have found that, when structural protons are removed, the Keggin anions start to converge and deform. This process is accompanied by an exothermic effect at 435°C. A  $\text{PMo}_{12}\text{O}_{38.5}$  phase is formed. A reversible transformation of the phase to parental acid during its dissolving or long storage in wet air shows its anhydride HPA properties. For the mixed P–Mo–V HPA, the “anhydride-like”

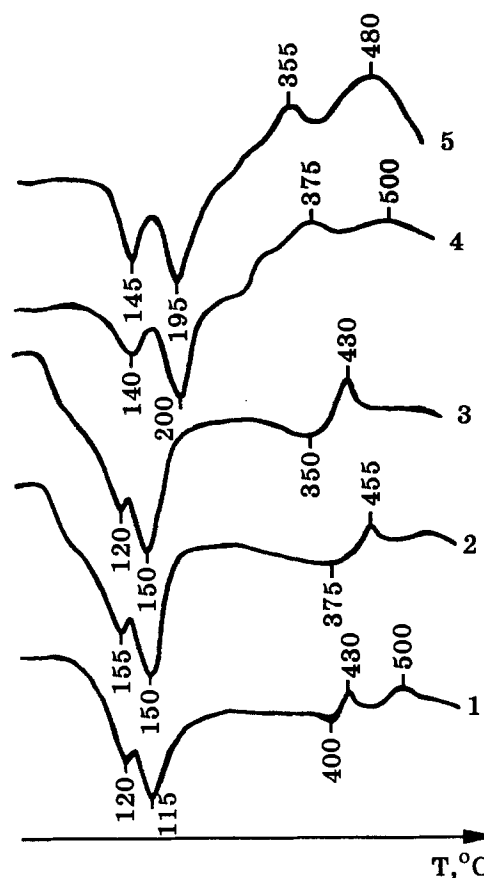


Fig. 1. DTA curves of  $\text{H}_3\text{PMo}_{12}\text{O}_{40} \cdot 13\text{H}_2\text{O}$  (1);  $\text{H}_4\text{PV}_1\text{Mo}_{11}\text{O}_{40} \cdot 14\text{H}_2\text{O}$  (2);  $\text{H}_5\text{PV}_2\text{Mo}_{10}\text{O}_{40} \cdot 14\text{H}_2\text{O}$  (3);  $\text{Na}_7\text{PV}_4\text{Mo}_8\text{O}_{40} \cdot 14\text{H}_2\text{O}$  (4) and  $\text{Na}_8\text{HPV}_6\text{Mo}_6\text{O}_{40} \cdot 7\text{H}_2\text{O}$  (5).

compounds also form [17]. Their formation is accompanied by an exothermic effect. Such compounds can recover to HPA in dissolving as well.

The displacement of the exothermic effect (fig. 1) evidences that the thermal stability of mono-vanadium HPA is higher than that of P–Mo HPA, while a further increase in vanadium content slightly decreases the stability. Our results comply with the other data obtained in refs. [17,22,26].

Since the reaction temperature in the catalytic measurements does not exceed 400°C, we may expect that the Keggin anion should retain in HPA, as the catalytic activity is measured. Fig. 2 shows the IR spectra of the samples before and after reaction. Within 400–1200  $\text{cm}^{-1}$ , which is the range characterizing the Keggin anion [27,28], the spectra of P–Mo and P–Mo–V HPA after reaction are similar to those before (fig. 2, spectra 1–6). Thus the primary HPA structure does not change in the reaction course. However, the secondary structure and phase composition change noticeably. Thus the IR spectra show the band at 1405–1410  $\text{cm}^{-1}$  typical for  $\delta_{\text{asNH}_4^+}$ . Therefore, ammonia salts of P–Mo and P–Mo–V HPA can form in the methylpyrazine ammoxidation. This is confirmed also by X-ray phase analysis. The X-ray patterns of P–Mo HPA before and after reaction (see

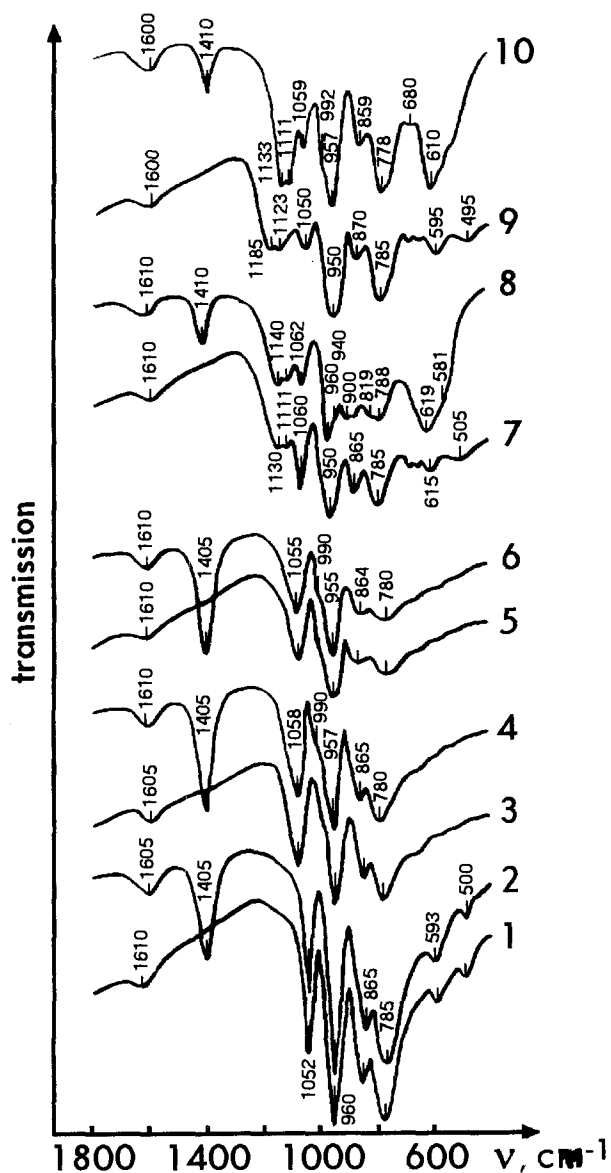


Fig. 2. IR spectra of  $H_3PMo_{12}O_{40}$  (1, 2),  $H_4PV_1Mo_{11}O_{40}$  (3, 4);  $H_5PV_2Mo_{10}O_{40}$  (5, 6);  $Na_7PV_4Mo_8O_{40}$  (7, 8) and  $Na_3HPV_6Mo_6O_{40}$  (9, 10). Initial samples (1, 3, 5, 7, 9) and samples after reaction (2, 4, 6, 8, 10).

fig. 3) are typical for the  $H_3PMo_{12}O_{40} \cdot 13H_2O$  of a monoclinic structure [29] and for the ammonia HPA salt of a cubic structure [30] respectively. The phase composition of mixed P–Mo–V HPA changes in the similar manner. They convert into the ammonia salts of the corresponding acids.

Fig. 4 shows the dependencies of methylpyrazine conversion, reaction product selectivity and carbon balance on reaction temperature for P–Mo HPA. Similar dependencies are also obtained for other heteropoly compounds. Table 1 shows the experimental results obtained.

In all samples carbon is not in balance when reaction temperature is lower than  $350^\circ C$ . We attribute such a low-temperature imbalance to the irreversible methyl-

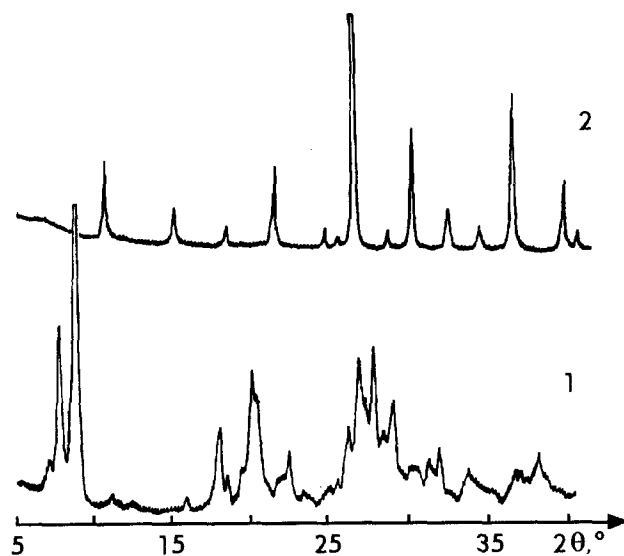


Fig. 3. X-ray patterns of P–Mo HPA before (1) and after reaction (2).

pyrazine adsorption on the strong acid proton sites. As reaction temperature increases, carbon balance increases due to the decrease of the Brønsted acid site number and their strength on dehydration [18] (causing the loss of structural water) and due to ammonia salts produced in the reaction of protons with ammonia of the reaction mixture.

In the balance experiments the increase of methylpyrazine conversion yields a slight decrease in the selectivity towards cyanopyrazine and a simultaneous increase in the selectivity towards pyrazine and  $CO_x$ . This confirms cyanopyrazine after-oxidation to occur. If methylpyrazine conversion is 80% and higher, the amount of  $CO_x$  exceeds that of pyrazine, thus evidencing the destruction of the heteroaromatic ring.

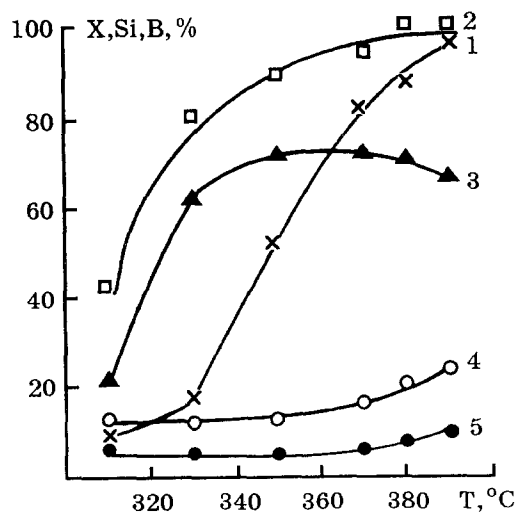


Fig. 4. Methylpyrazine conversion (1), carbon balance (2); and selectivities towards cyanopyrazine (3), pyrazine (4) and carbon dioxides (5) as functions of temperature.

Table 1  
Catalytic properties of heteropoly compounds at the methylpyrazine ammoxidation,  $\tau = 2$  s

Catalyst composition (surface)	$T_r$ (°C)	$X$ (%)	$K^I$ (s <sup>-1</sup> )	Selectivity (%)			$B^a$ (%)	Yield (%) C <sub>5</sub> H <sub>3</sub> N <sub>3</sub>
				CO <sub>x</sub>	C <sub>4</sub> H <sub>4</sub> N <sub>2</sub>	C <sub>5</sub> H <sub>3</sub> N <sub>3</sub>		
H <sub>3</sub> PMO <sub>12</sub> O <sub>40</sub> ( $S = 2$ m <sup>2</sup> /g)	310	9.6	0.05	7.1	12.9	21.8	41.8	2.1
	330	17.0	0.09	5.3	12.5	62.9	80.7	10.7
	350	52.3	0.37	4.7	13.2	71.7	89.6	34.5
	370	82.1	0.86	6.0	16.8	72.9	95.7	59.8
	380	87.5	1.02	7.7	20.5	71.4	99.6	62.5
	390	97.3	1.81	9.2	24.3	67.1	100.6	65.3
H <sub>4</sub> PV <sub>1</sub> Mo <sub>11</sub> O <sub>40</sub> ( $S = 2.1$ m <sup>2</sup> /g)	300	14.4	0.02	5.5	8.7	29.1	43.3	4.2
	320	30.4	0.18	4.3	7.8	44.3	56.4	13.5
	345	56.6	0.42	5.5	8.3	70.8	84.6	40.1
	355	74.5	0.68	6.3	6.7	84.8	97.8	63.2
	365	81.1	0.94	5.1	6.8	83.7	95.6	67.9
	375	92.7	1.31	5.8	7.0	83.0	95.8	76.9
	385	94.7	1.91	15.8	19.8	63.0	98.6	59.7
	H <sub>5</sub> PV <sub>2</sub> Mo <sub>10</sub> O <sub>40</sub> ( $S = 2.8$ m <sup>2</sup> /g)	310	30.5	0.18	7.8	10.5	50.3	68.6
330		57.1	0.42	5.4	8.4	46.3	60.1	26.4
350		79.0	0.78	6.3	13.5	74.4	94.2	58.8
360		90.0	1.15	5.3	10.9	83.2	99.4	74.9
380		97.5	1.84	6.4	11.1	79.3	96.8	77.3
390		98.1	1.98	7.2	12.9	78.6	98.7	77.1
Na <sub>7</sub> PV <sub>4</sub> Mo <sub>8</sub> O <sub>40</sub> ( $S = 1.8$ m <sup>2</sup> /g)		300	18.7	0.10	2.3	2.9	22.4	27.6
	320	24.7	0.14	2.3	4.8	29.6	36.7	7.3
	340	43.3	0.28	2.4	4.6	49.6	56.6	21.5
	360	51.7	0.36	2.6	7.2	66.7	76.5	34.5
	380	64.1	0.51	3.7	7.9	79.2	90.8	50.8
	390	89.0	1.10	4.0	16.9	73.9	94.8	65.8
	400	98.5	2.10	5.2	22.6	72.2	100.0	71.1
	Na <sub>8</sub> HPV <sub>6</sub> Mo <sub>6</sub> O <sub>40</sub> ( $S = 1.8$ m <sup>2</sup> /g)	290	16.7	0.09	2.2	3.8	5.3	11.3
310		22.6	0.13	2.1	4.1	29.1	35.3	6.6
320		28.3	0.17	2.7	3.6	38.7	45.0	11.0
340		35.4	0.22	2.5	3.8	51.3	57.6	18.2
360		47.1	0.32	2.2	5.6	69.1	76.9	32.5
380		62.3	0.49	4.2	10.9	80.5	95.6	50.2
390		91.4	1.23	5.4	12.7	80.5	98.6	73.6
400		98.3	2.04	5.7	16.6	75.7	98.0	74.4

<sup>a</sup> B: balance.

Basing on our experimental data, we believe that methylpyrazine ammoxidation follows the same consecutive-parallel scheme as in the case of oxide catalysts [14]:

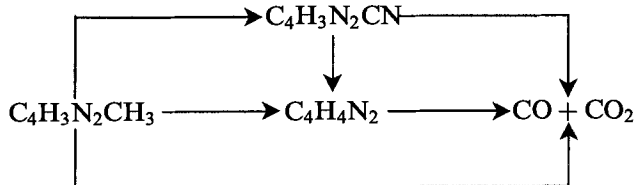


Fig. 5 compares the catalytic properties of samples, regarding vanadium atom content in the Keggin anion. Vanadium introduction instead of one or two molybdenum atoms is accompanied by the increase in both activity and selectivity towards cyanopyrazine, the substitution of the first molybdenum atom strongly affecting catalysis. Further substitutions have no signifi-

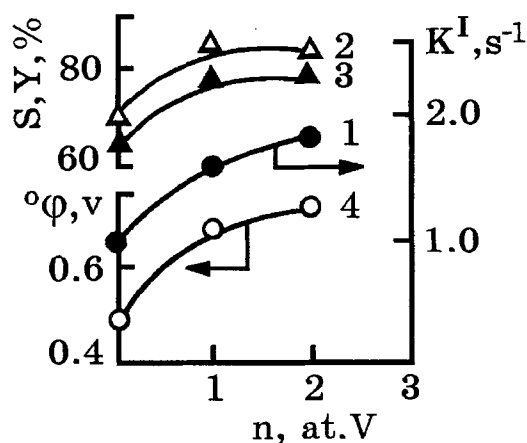


Fig. 5. Relationship between activity (1), selectivity towards cyanopyrazine at a 90% conversion (2), maximal cyanopyrazine yield (3) and oxidation potential (4) and V content in the samples.

Table 2

Effect of reaction time on the catalytic properties of P-Mo HPA.  $T_r = 390^\circ\text{C}$ , contact time  $\tau = 1$  s

Reaction time (h)	X (%)	Selectivity (%)			Carbon balance (%)
		CO <sub>x</sub>	C <sub>4</sub> H <sub>4</sub> N <sub>2</sub>	C <sub>5</sub> H <sub>3</sub> N <sub>3</sub>	
1	65.1	5.4	16.1	75.0	96.5
5	65.4	5.0	15.1	76.2	96.3
16	64.0	5.3	15.7	77.0	98.0
22	63.7	4.5	15.3	76.7	96.5
26	64.1	5.2	16.4	75.4	97.0
36	63.7	5.4	16.5	74.0	95.9

cant effect. Stronger oxidative properties may be a factor increasing the activity and selectivity towards cyanopyrazine as vanadium is introduced. Fig. 5 also shows the literature data [19] on the HPA oxidative potential ( $^\circ\varphi$ ) as a function of composition. It is evident that the curves change in a symbatic manner.

The catalytic properties of P-Mo-V HPA can also be improved by a more efficient methylpyrazine activation on vanadium-containing active sites [20].

Vanadium similarly affects the HPA activity and selectivity in the oxidation of acrolein, isobutylene and isobutane to the corresponding acids [21,22,26].

Since the catalytic reaction occurs at temperatures close to the stability temperature for the Keggin anions P-Mo and P-V-Mo (HPA), samples can be deactivated in the reaction course due to the HPA decomposition caused by the high temperature and reducing reaction medium.

Table 2 presents the data showing how the catalytic properties depend on the time of reaction over P-Mo HPA, which is the least thermally stable acid among the studied ones. Long time experiments were performed with the sample after the step-wise reaction temperature increase from 300 to 390°C. The table shows that neither activity nor selectivity change significantly. Thus we believe that such a behavior is due to the ammonia salts (forming in the presence of ammonia) that are more stable than the corresponding HPA [23].

### 3.2. Sodium HPA salts

The dehydration of Na<sub>7</sub>PV<sub>4</sub>Mo<sub>8</sub>O<sub>40</sub> and Na<sub>8</sub>HPV<sub>6</sub>Mo<sub>6</sub>O<sub>40</sub> salts proceeds somewhat different. Water and proton removal causes secondary structure rearrangement and the cubic-structure salts produced undergo crystallization, which is accompanied by the exoeffect at 355–375°C (fig. 1, curves 4 and 5). These salts start to decompose just after crystallization ends. The maximum temperatures of the corresponding exothermal peaks of Na<sub>7</sub>PV<sub>4</sub>Mo<sub>8</sub>O<sub>40</sub> and Na<sub>8</sub>HPV<sub>6</sub>Mo<sub>6</sub>O<sub>40</sub> salts equal 500 and 480°C, respectively. Thus within 300–400°C we may expect a partial decomposition of heteropoly anions in the reaction course.

Indeed after reaction performance, beside the lines typical for cubic structure HPA salts [30] the X-ray patterns show the lines corresponding to the mixed sodium vanadium molybdates such as Na<sub>2</sub>VMoO<sub>6</sub> identified according to ref. [31]. The IR spectra of the salts show the band shifts within 1100–1200 cm<sup>-1</sup>, some bands within 600–670 cm<sup>-1</sup> disappear and new bands appear within 800–990 cm<sup>-1</sup> (see fig. 2, spectra 7–10). This fact also evidences a partial decomposition of the HPS.

Table 1 shows that sodium salts are somewhat less active and selective than the catalysts based on the P-Mo and P-Mo-V HPA.

The change of activity and selectivity of salts towards reaction products with increasing temperature is similar to that already described. At comparatively low temperatures the change is caused by dehydration and secondary structure rearrangements producing mixed sodium-ammonia salts. At high temperatures the Keggin anions partially decompose, and thus phase composition changes.

In conclusion, let us note that HPA used as catalysts in the ammoxidation of methylpyrazine allow a 75–77% yield of cyanopyrazine. This yield is close to that described in the patents concerning the oxide catalysts [24,25].

### References

- [1] Y. Ono, in: *Perspectives in Catalysis*, eds. J.M. Thomas and K.I. Zamaraev (Blackwell, Oxford, 1992).
- [2] I.V. Kozhevnikov and K.I. Matveev, *Usp. Khim.* 52 (1982) 1433.
- [3] M. Misono, *Catal. Rev. Sci. Eng.* 29 (1987) 269.
- [4] V.F. Chuvayev, A.I. Gasanov and V.I. Spitsyn, *Auth. Certificate No. 550373*, BI 1977, 10.
- [5] M.A. Schwegler and H. van Bekkum, *Bull. Soc. Chim. Belg.* 99 (1990) 113.
- [6] G.B. McGarvey and J.B. Moffat, *J. Catal.* 132 (1991) 100.
- [7] M. Misono and N. Nojiri, *Appl. Catal.* 64 (1990) 1.
- [8] I.V. Kozhevnikov, *Usp. Khim.* 62 (1993) 510.
- [9] L. Forni, *Appl. Catal.* 20 (1986) 219.
- [10] Sh. Shimizu, T. Nivu and T. Shoji, *Catalyst* 33 (1991) 386.
- [11] L. Forni, C. Oliva and C. Rebuschini, *J. Chem. Soc. Faraday Trans. I* 84 (1988) 2397.
- [12] A.D. Kagarlitskii, L.A. Krichevskii and B.V. Suvorov, *Khim. Farmats. Zh.* 3 (1993) 45.

- [13] N.A. Polotebnova, Nguen Van Cheu and V.V. Kal'nibolotskaya, *Zh. Neorg. Khim.* 18(1973)413.
- [14] V.M. Bondareva, T.V. Andrushkevich and G.A. Zenkovets, *Kinet. Katal.*, in press.
- [15] Kh.I. Lunk, V.F. Chuvayev and V.I. Spitsyn, *Dokl. Akad. Nauk SSSR* 247(1978) 121.
- [16] V.M. Bondareva, T.V. Andrushkevich, R.I. Maksimovskaya, L.M. Plyasova, A.V. Ziborov, G.S. Litvak and L.G. Detusheva, *Kinet. Katal.* 35(1994) 129.
- [17] H.G. Jerchkewitz, E. Alsdorf and H. Fischer, *Z. Anorg. Allg. Chem.* 526(1985) 73.
- [18] E.M. Serwicka, K. Bruckman, J. Haber, E.A. Paukshtis and E.N. Yurchenko, *Appl. Catal.* 73(1991) 153.
- [19] V.F. Odyakov, L.I. Kuznetsova and K.I. Matveev, *Zh. Neorg. Khim.* 23(1978) 457.
- [20] I.G. Iovel, M.V. Shimanskaya and L.Ya. Margolis, *Izv. Akad. Nauk Latv. SSR, Ser. Khim.* 3(1977) 319.
- [21] K. Bruckman, J. Haber, E. Lalic and E.M. Serwicka, *Catal. Lett.* 1(1988) 35.
- [22] G. Lischke, R. Ecket and G. Ohlmann, *React. Kinet. Catal. Lett.* 31(1986) 267.
- [23] E.N. Yurchenko, L.G. Detusheva, I.P. Olen'kova, O.I. Goncharova and G.S. Litvak, *Izv. SO RAN SSSR* 1986, No. 8, Ser. Khim. Nauk, vyp. 5, p. 51.
- [24] FRG Patent: 3107756.
- [25] US Patent: 4931561.
- [26] G. Centi, J.L. Nieto, C. Iapalucci, K. Bruckman and E.M. Serwicka, *Appl. Catal.* 46(1986) 197.
- [27] C. Rocchiccioli-Deltcheff, R. Thouvenot and R. Franck, *Spectrochim. Acta* 32A(1976) 587.
- [28] E.N. Yurchenko and L.G. Detusheva, *Zh. Strukturnoy Khimii* 23(1982) 66.
- [29] ASTM 9-412.
- [30] ASTM 21-1380.